DOI: 10.1002/cbic.200800769

A Peptide Antagonist of the TLR4–MD2 Interaction

Peter F. Slivka,[a] Mitesh Shridhar,[a] Gui-in Lee,[c] Deanne W. Sammond,[a] Mark R. Hutchinson,[b] Alexander J. Martinko,[a] Madison M. Buchanan,[a] Page W. Sholar,[b] Jeffrey J. Kearney,[b] Jacqueline A. Harrison,[b] Linda R. Watkins,[b] and Hang Yin*[a]

Toll-like receptor 4 (TLR4) is a toll-like receptor (TLR) family protein that organizes an innate immune response that distinguishes nonself and endogenous danger signals.[1] Specifically, TLR4 recognizes lipopolysaccharide (LPS) from the cell wall of Gram-negative bacteria, as well as endogenous signals such as HSP60, HSP70, and fibrinogen.[2] Agonism of the receptor is dependent upon a homodimeric TLR4 signaling complex that includes myeloid differentiation factor 2 (MD2).[3] The assembly of the TLR4–MD2 complex initiates a MyD88-dependent signaling cascade, which relocates nuclear factor-κB (NF-κB) from the cytoplasm to the nucleus.[4] Transcription by the NF-κB promoter directs the production of a number of proinflammatory cytokines including TNFα, IL-1β, IL-6, and IFN-γ.[2] Recent evidence suggests that TLR4-mediated elevations in the expression of these cytokines in glia cells and astrocytes in the central nervous system (CNS) initiate and propagate several debilitating disease states such as chronic pain and sepsis.[5–7] The lack of good clinical treatments for chronic pain has made its effectors, including TLR4, popular targets for new therapeutics.[5]

Chronic pain occurs in epidemic proportions worldwide.[8] The disease typically arises from two types of injuries: 1) tissue injuries that lead to inflammatory pain, and 2) nerve injuries that lead to neuropathic pain. Microglia in the CNS recognize a variety of signals associated with inflammatory or nerve injury and subsequently release a variety of inflammatory mediators in response, including TNFα, IL-1β, IL-6, PGE-2, COX-2, and ATP. The release of these molecules stimulates other glia to respond in a proinflammatory manner, and also results in neuronal actions. Stimulation of nociceptive pain neurons by glial inflammatory mediators leads to hypersensitivity and enhanced pain states. This centrally mediated pathological pain causes exaggerated pain sensitivity in healthy and undamaged tissues. The hypersensitive state leads to intense and exaggerated pain being sensed from both painful (hyperalgesia) and/or nonpainful stimuli (allodynia).[2,8]

Previous research has indicated that TLR4 plays a major role in the development of chronic pain.[9–11] TLR4 is now well documented to become activated by so-called "endogenous danger signals". These are substances released by stressed or damaged cells (such as the HMGB-1, and HSP proteins, etc.) that signal distress of host cells through TLR4 signaling, which leads to glial release of proinflammatory mediators. In fact, TLR4-knockout mice that have undergone nerve injury do not develop allodynia and show reduced glial activation with lower levels of pain-related mediators.[12] Moreover, hypersensitivity can be attenuated in chronic pain rats by using a TLR4 antisense oligonucleotide.[12]

TLR4 signaling is dependent upon the formation of a homodimer, which is mediated by the accessory protein MD2.[13,14] Specific point mutations to MD2 (for example, Cys95Tyr), which prevent its association with TLR4, significantly diminishes TLR4 signaling.[15] TLR4-based peptides or TLR4-MD2 fusion proteins can also attenuate signaling by competing for MD2 or LPS respectively .[16,17] Given the wide array of agonists that TLR4 recognizes, it is not clear whether a peptide that targets TLR4 directly would agonize or antagonize the receptor. The recently reported high-resolution X-ray crystal structure of the murine TLR4–MD2 complex revealed several molecular recognition sites on the TLR4–MD2 interface that could serve as potential targets for a peptide.[18] A charged patch spanning from Asp99 to Glu111 (critical charged residues are underlined in Table 1) of MD2 was projected to be critical to the nanomolar binding affinity of MD2 and TLR4. These charged residues are projected by a short α helix (Ser103–Lys109) and a random-coil protruding loop (Cys95–Tyr102) that is constrained by a disulfide bridge between Cys95 and Cys105. Herein, we employed a chemical biology approach by utilizing the minimal TLR4-binding region of MD2 to block the TLR4–MD2 association. The in silico, in vitro, and whole-cell data demonstrated for the

[a] *P. F. Slivka, M. Shridhar, Dr. D. W. Sammond, A. J. Martinko, M. M. Buchanan, Prof. Dr. H. Yin*
Department of Chemistry and Biochemistry
215 UCB, University of Colorado
Boulder, CO 80309-0215 (USA)
Fax: (+1) 303-492-5894
E-mail: hang.yin@colorado.edu

[b] *Dr. M. R. Hutchinson, P. W. Sholar, J. J. Kearney, J. A. Harrison, Prof. Dr. L. R. Watkins*
Department of Psychology, 345 UCB, University of Colorado
Boulder, CO 80309-0215 (USA)

[c] *Prof. Dr. G.-i. Lee*
Department of Chemistry, The Pennsylvania State University
Abington, PA 19001 (USA)

Supporting information for this article is available on the WWW under http://dx.doi.org/10.1002/cbic.200800769.

Table 1. Sequence alignment of human and murine MD2. Underlined residues are identified as critical binding residues. Disulfide-forming cysteines are highlighted in bold. The italicized residue is mutated in the negative control.

Name	Sequence
human[a]	R^{90}KEVI**C**RGSDDDYSF**C**RALKGETVNTTISFS^{120}
murine[a]	R^{90}KEVL**C**HGHDDDYSF**C**RALKGETVNTSIPFS^{120}
MD2-I	**C**RGSDDDYSF**C**RALKGE
MD2-II	*A*RGSDDDYSF**C**RALKGE

[a] Sequence alignment from Kim et al.[18]

first time that an MD2-based peptide inhibitor can suppress the TLR4 signaling in live cells; this suggests novel strategies of using peptidomimetic and small-molecule agents to target a variety of CNS disorders.

A 17-residue peptide (MD2-I) was synthesized to reproduce the TLR4-binding region of the MD2 protein that contains all the critical interacting residues (Table 1). We rationalized that the disulfide bridge between Cys95 and Cys105 and the secondary structures of the peptide help to retain the geometry of the critical residues in 3D space and mimic that of the TLR4-binding regions of the full-length MD2. Previous studies with MD2 mutants showed that the disulfide-forming Cys95 residue is critical for MD2 binding TLR4.[15] As such, a mutant MD2-I peptide (MD2-II) with Cys95 replaced with an Ala residue was also synthesized. Formation of the disulfide bond in MD2-I was verified with mass spectrometry (Figure S2 in the Supporting Information). Further, circular dichroism (CD) experiments were performed to determine if MD2-I retained the structural features of full-length MD2. In the presence of 10–30% trifluoroethanol (TFE) in aqueous solution, the CD spectra of MD2-I and II show α-helical characteristics with two negative peaks at 208 and 222 nm (Figure S3). This demonstrates that the truncated peptides retain the secondary structures of the full-length MD2. Because both peptides are observed to have similar secondary structures, their binding modes to TLR4 are expected to be the same, which allows the direction comparison of their inhibitory potency to be made.

To determine if the truncated MD2 sequence would retain its affinity for TLR4, the binding energy of MD2-I and full-length MD2 were first computed by using Rosetta in the interface mode (Table S1). MD2-I has a slightly higher affinity ($\Delta G = -7.8$ kcal mol^{-1}) than the full-length MD2 ($\Delta G = -5.5$ kcal mol^{-1}) when docked against a truncated version of the human TLR4 receptor (PDB ID: 2z65). When docked against a humanized version of the full-length, murine TLR4 receptor (PDB ID: 2z64) the affinity of MD2-I ($\Delta G = -7.1$ kcal mol^{-1}) was slightly lower than the affinity of full-length MD2 ($\Delta G = -9.1$ kcal mol^{-1}). Collectively, these computational simulations predicted that MD2-I should retain some affinity for TLR4, thereby competing with the full-length MD2 for the TLR4-binding site. (Figure 1)

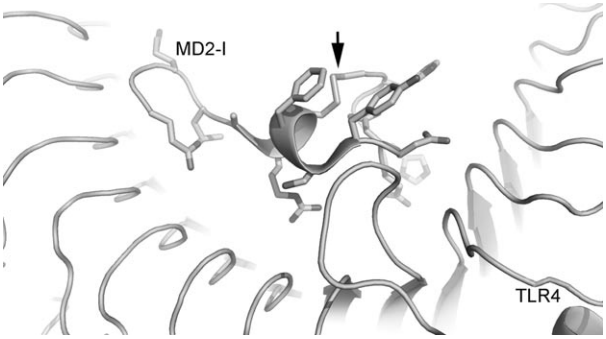

Figure 1. Computationally simulated protein–protein interface between TLR4 and MD2-I suggesting that MD2-I adopts a similar conformation to the TLR4-binding region of MD2. The constraint disulfide bridge marked by an arrow.

The inhibitory effects of MD2-I on lipopolysaccharide (LPS), a native ligand of the TLR4–MD2 complex, was studied in live, stably transfected HEK293 cells that express TLR4 along with its accessory proteins. Cells were incubated with 10 μg mL^{-1} LPS that was conjugated with fluorescein isothiocyanate (LPS-FITC) in the absence or presence of the MD2 peptides and scanned in a flow cytometer. Cells that were incubated for two hours with LPS-FITC only show a half-decade shift downfield, which is indicative of LPS-FITC binding to the TLR4–MD2 complex on the cell membrane. Cells that were co-incubated with LPS-FITC and 0.1 mM MD2-I show almost no shift after two hours; this suggests that MD2-I blocks LPS-FITC binding to the TLR4–MD2 complex (Figure 2). Cells that were co-incubated

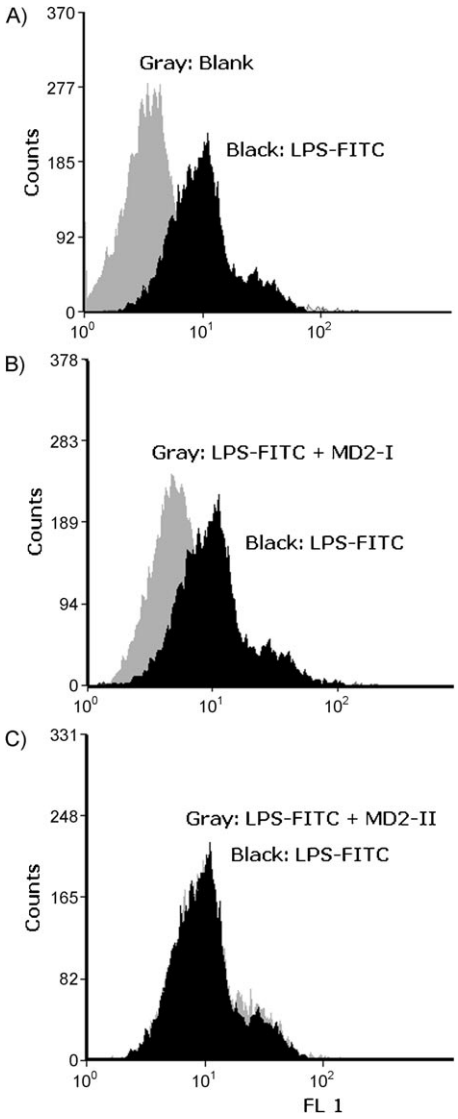

Figure 2. Flow cytometry results showing the binding of TLR4-overexpressing HEK293 cells binding to LPS-FITC in the presence and absence of peptide inhibitors. A) Overlay of native HEK293 cells (gray) and HEK293 cells incubated with 10 μg mL^{-1} LPS-FITC (black). B) Overlay of HEK293 cells incubated with 10 μg mL^{-1} LPS-FITC (black) and co-incubated with 10 μg mL^{-1} LPS-FITC and 0.1 mM MD2-I (gray). C) Overlay of HEK293 cells incubated with 10 μg mL^{-1} LPS-FITC (black) and co-incubated with 10 μg mL^{-1} LPS-FITC and 0.1 mM MD2-II (gray).

with LPS-FITC and MD2-II show a half-decade shift downfield that is analogous to the shift that was seen with LPS-FITC alone; this indicates that MD2-I behaves similarly to Cys95Tyr MD2 mutants. Together these data suggest that MD2-I not only blocks the binding of LPS to TLR4-expressing cells, but also behaves in a similar fashion to MD2 and its mutants; this suggests that MD2-I is in fact blocking the TLR4–MD2 interaction.

MD2-I is also shown to be effective at blocking the downstream proinflammatory effectors of TLR4 in HEK293 cells and murine macrophages. The same HEK293 cells that stably express TLR4 also contain a secreted alkaline phosphatase reporter gene (SEAP) located downstream from the NF-κB promoter.[19] These cells were treated with a gradient of LPS ranging from 0.01 to 100 ng mL^{-1} and a constant 0.1 mM dose of MD2-I or MD2-II (Figure 3). Cells that were incubated with LPS show

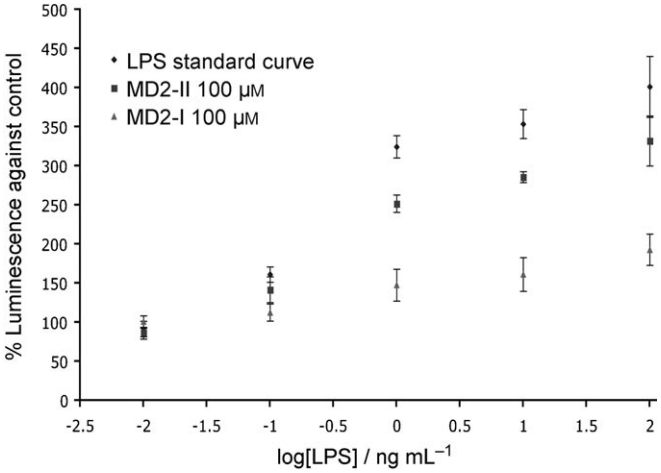

Figure 3. SEAP reporter gene activity with MD2-I (triangles) and MD2-II (squares) compared to blank control (diamonds). Confluent cells in 96-well plates were incubated with LPS (0.01 ng mL^{-1} to 100 ng mL^{-1}) or co-incubated with LPS and MD2-II (0.1 mM) or MD2-I (0.1 mM) in CSF buffer for 24 h. SEAP levels were quantitated by using Applied Biosystems Phospha-Light Chemiluminescent Reporter Gene Assay System according to manufacturer specifications. Samples were detected on a Beckman Coulter, DTX 880 plate reader with 1000 ms integration time per well. Data are expressed as % luminescence against a control sample that contains only buffer and peptide.

a level of SEAP activation that ranges from 89% at low concentration to 401% at high concentration when compared to a blank control. Cells that were co-incubated with MD2-II show slightly reduced levels of activation (87–332%), but cells treated with MD2-I show significantly reduced levels of activation (101–193%). These results demonstrate that MD2-I, but not the control peptide MD2-II, blocks LPS-induced activation. Furthermore, the reduced level of maximum TLR4 activation in the presence of MD2-I indicates that MD2-I blocks LPS binding as a non-competitive inhibitor. This result is consistent with MD2-I targeting an allosteric site of the TLR4–MD2 association, lending further support to the peptide inhibitor design.

In addition to the NF-κB pathway, LPS activation of TLR4 has also been shown to activate phosphoinositide 3 kinase (PI3K); this triggers translocation of Akt1 to the plasma membrane in murine macrophages.[20] Murine MD2 has two mutations in the C95–E111 binding loop (Arg96His, Ser98His). Neither of them have been identified as critical residues in the TLR4–MD2 interaction, which suggests that human MD2 peptides should function properly in a murine model.[18] RAW 264.7 cells transfected with an Akt1-GFP reporter[21] were treated with MD2-I and MD2-II then activated with LPS. In the absence of LPS, Akt1-GFP is uniformly diffused throughout the cytosol (Figure S4A). Addition of LPS causes a rapid translocation of Akt1-GFP to the plasma membrane lowering Akt1-GFP concentration in the cytosol. Cells that were treated with MD2-I show almost no change in Akt1-GFP diffusion when LPS is added (Figure 4A and Figure S4C). A small dose of complement 5a (C5a, 25 ng mL^{-1}) confirms that these cells were active, but their ability to signal through TLR4 was inhibited (Figure S4D). MD2-II did not show the same ability to block TLR4 agonism. After addition of LPS, these cells showed a very similar activation profile to untreated cells (Figure 4B). These data concur with the SEAP reporter gene studies in a more complex system. Because Akt1 is right downstream of TLR4 in the signal transduction pathway,[20] these data provide strong evidence that MD2-I

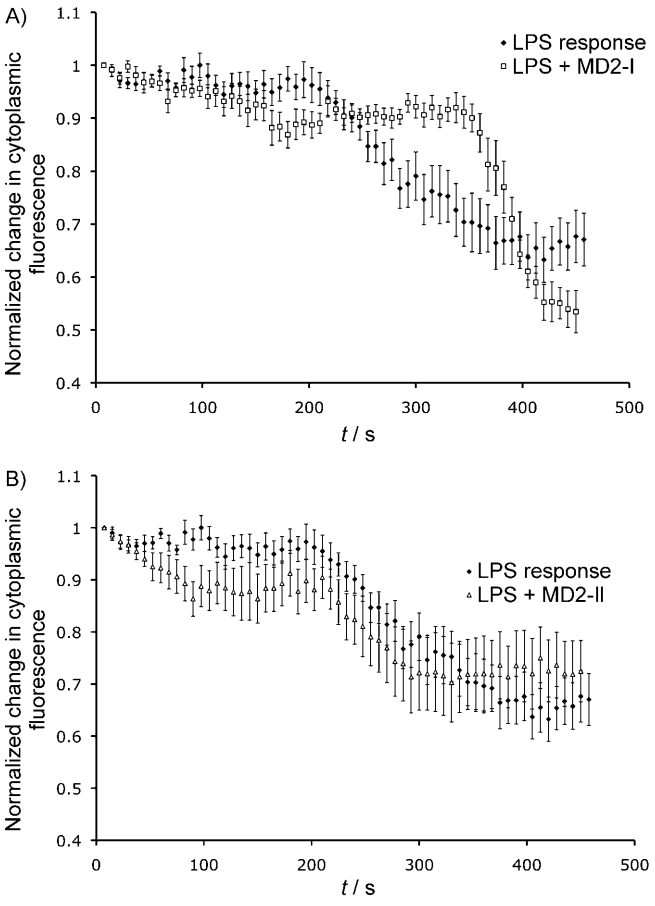

Figure 4. Comparison of MD2-I and MD2-II inhibition of LPS-induced TLR4 activation. Murine macrophages were treated with 100 μM A) MD2-I (□) or B) MD2-II (△) at 35 s. After two and a half minutes LPS was added to a final concentration of 200 ng mL^{-1}. If no visual response was observed after an additional two and a half minutes C5a (25 ng mL^{-1}) was added to confirm that the cells were responsive (A). LPS response curve (◆) was collected with no peptide pretreatment.

blocks TLR4-mediated signaling by directly interacting with TLR4. Murine macrophages express a variety of TLRs and immune receptors. Inhibiting LPS-induced agonism of TLR4 suggests that MD2-I is specific for TLR4 over other TLRs.

In summary, we have demonstrated that a short peptide corresponding to the TLR4-binding loop can prevent the full-length MD2 from binding to TLR4. Subsequently, the peptide can inhibit LPS-induced expression of proinflammatory cytokines, which are linked to TLR4 agonism both in human cells and in murine cells. By using a Cys95Ala mutant of MD2-I, we have shown that the activity of the peptide correlates well with full-length MD2 mutants; this suggests that the peptide is specifically blocking the TLR4–MD2 interaction. These studies pave the way for the development of more drug-like small-molecule peptidomimetic antagonists of TLR4, which might eventually find applications in drug discovery.

Experimental Section

Peptide synthesis: All peptides were synthesized in the CEM Discover microwave by using the standard FMOC chemistry that was outlined by Bacsa and Kappe with modifications.[22] Three equivalents of HCTU coupling reagent (Pepnet, Louisville, KY, USA) and three equivalents of amino acid (ChemPep, Miami, FL, USA) were used per coupling. Each coupling was performed in duplicate and coupling times were reduced to 2 min. After cleavage and workup, peptides were characterized by using Perseptive Biosystems MALDI-TOF Mass Spectrometer. Purification of peptides was carried out on a Waters 600E HPLC equipped with a SepaxGP-C8 reversed-phase, 21.2×250 mm column over a 50:50 to 0:100 (H_2O, 0.1% TFA/acetonitrile, 0.1% TFA) gradient for 30 min. Fractions were characterized with MALDI mass spectrometry and lyophilized to dryness.

Computational studies: Human-specific interface sequence positions (TLR4: F160L, G234N, K263R, D264N, T290A MD2: H96R, H98R) were modeled onto the murine TLR4–MD2 complex by using the alignment provided by Kim et al. to investigate structural differences. Binding energy calculations and side-chain simulations were performed with the molecular modeling program Rosetta,[23] in which low-energy combinations of side-chain conformations were identified by using Monte Carlo optimization with simulated annealing.[24] Binding energies were calculated by subtracting the calculated energy of each unbound protein from the calculated energy of the complex. The side-chain conformations of the mutated residues were built by choosing the rotamer with the lowest energy when modeled in the context of the complex. Neighboring side-chains and backbone conformations were held fixed in the positions that were observed in the crystal structure. For the modeling described here, a version of the energy function that significantly dampens repulsion energies to allow for small atom–atom clashes that might be accommodated by small changes in side-chain and backbone conformation was used. It is referred to as Rosetta_DampRep.[25] Dunbrack's backbone-dependent rotamer library supplemented with rotamers that vary $\chi1$ and $\chi2$ one standard deviation away from their most probable values was also used in these calculations.[26]

Circular dichroism studies: Far-UV circular dichroism spectra were collected in 0.1 cm quartz cells by using a Jasco J-810 spectropolarimeter at 25 °C. The cuvette holder had a temperature controller with the external temperature probe. Scanning was performed in step-scanning mode with a 4 s response time. The CD signals were averages of three repeated scans with 1 nm/sec spacing from 260 to 190 nm. Baseline correction was done by using the solvent-only scans. Solvent for CD experiments were 30% TFE in H_2O. The MD2-I (95 μM) of the peptides was calculated by the UV absorbance at 280 nm with the extinction coefficient 1615 $M^{-1}cm^{-1}$ and 1490 $M^{-1}cm^{-1}$. The data were converted to mean residue ellipticity $[\theta]$ in deg cm^2 $dmol^{-1}$ by using the equation $[\theta]=(\theta_{obs}/10Lc)/r$, where θ_{obs} is the ellipticity measured in millidegrees, l is the optical path length (cm), c is the concentration of the peptide (M), and r is the number of residues.

Flow cytometry: Cells were lifted on the day of experiment and centrifuged at 1000 rpm for 5 min. Medium was decanted and replaced with cerebral spinal fluid (CSF) buffer (124 mM NaCl, 5 mM KCl, 0.1 mM $CaCl_2$, 3.2 mM $MgCl_2$, 26 mM $NaHCO_3$, and 10 mM glucose, pH 7.4) to a final concentration of 1×10^6 cells mL^{-1}. Cells were aliquoted (800 μL per tube) into 5 mL sorter tubes (Becton Dickinson, Franklin Lakes, NJ, USA) and coincubated with of 100 ng mL^{-1} LPS-FITC (100 μL; Sigma) and H_2O (100 μL) or a 1 mM peptide solution (100 μL). After 2 h, flow data was collected by using a MoFlo DakoCytomation cell sorter that was equipped with a 488 nm argon laser. Summit Software v4.0 was used to collect and quantify the data. A total of ten thousand events were collected for each tube.

SEAP Assay: Human embryonic kidney 293 (HEK293) cells that were stably transfected with TLR4, necessary assembly and signaling proteins (MD2, CD-14, LPSBP, etc.) and a secreted alkaline phosphatase (SEAP) reporter gene were obtained from InvivoGen (HEK blue-4 cells; San Diego, CA, USA). Cells were cultured in DMEM supplemented with 10% FBS, penicillin (100 U mL^{-1}), streptomycin (100 μg mL^{-1}), L-glutamine (2 mM), 1× normocin (InvivoGen, ant-nr-1) and 2×HEK Blue selection (InvivoGen, hb-sel). Cells were implanted in 96-well plates 48 h prior to drug treatment and incubated at 37 °C. On the day of treatment, media was removed from the 96-well plate and replaced with CSF buffer that contained a mixture of LPS and peptide. After 24 h, a sample of CSF buffer (15 μL) from each well was collected and transferred to an opaque white 96-well plate (Microfluor 2, Thermo Scientific, Waltham, MA, USA). Each well was treated with 1× dilution buffer (45 μL), covered with a microseal (Bio-Rad, MSB1001, Hercules, CA, USA), and incubated for 30 min at 65 °C. After 30 min, plates were cooled to room temperature on ice and SEAP assay buffer (50 μL) was added to each well. After a 5 min incubation, disodium 3-(4-methoxyspiro{1,2-dioxetane-3,2′-(5′-chloro)tricyclo[3.3.1.1^{3,7}]decan}-4-yl) phenyl phosphate (50 μL; CSPD) diluted 1:20 with reaction buffer was added to each well. After 20 min, the luminescence of each well was measured by using a Beckman Coulter, DTX 880 plate reader (Fullerton, CA, USA) with Multimode Analysis Software. Raw luminescence scores were expressed as a percentage of luminescence against a control that contained only peptide.

Murine macrophage Akt1-GFP imaging: LPS-induced activation of Akt1-GFP was studied in RAW264.7 mouse macrophages. These cells were stably transfected to express GFP-tagged Akt1 and graciously provided by Dr. John Evans.[21] Cells were cultured in DMEM that was supplemented with 10% FBS, penicillin (100 U mL^{-1}), streptomycin (100 μg mL^{-1}), glutamine (0.292 mg mL^{-1}), and HEPES (20 mM) in 5% CO_2 at 37 °C and plated at 2×105 cells mL^{-1} 24 h prior to imaging on 3.5 cm MatTek glass-bottomed dishes. At the time of experiment, media was removed and cells were washed with HBSS (2×) that was supplemented with 25 mM HEPES buffered to pH 7.4. Conditioned HBSS (1.0 mL) was added to the cells for imaging. Media was conditioned by a 24 h incubation with

RAW264.7 cells. A Nikon inverted microscope with 60× oil immersion objective, GFP/RFP dichroic mirror, corresponding single-band excitation and emission filters, and CoolSNAP ES camera was used to carry out imaging. Excitation was provided with a mercury lamp. Images were taken every 7.5 s. Background fluorescence was captured for five frames. Peptides were added in a 200 μL dose to a final concentration of 100 μM. Twenty more frames were collected before 200 μL of LPS (200 ng mL^{-1} final) was added. If no visual response occurred after twenty frames, C5a (25 ng mL^{-1}) was added to the plates to confirm if the cells were responsive. Translocation of Akt1-GFP was quantified by using ImageJ and expressed as normalized change in cytoplasmic fluorescence (arbitrary units) over time.

Acknowledgements

We thank the Council on Research & Creative Work at the University of Colorado at Boulder for financial support of the work. P.F.S. thanks the University of Colorado Molecular Biophysics Training Grant (NIH T32 GM-065103) for support. M.R.H. is grateful for the Australian National Health and Medical Research Council C. J. Martin Fellowship (ID 465423), and L.R.W. thanks the National Institutes of Health (NIH DA017670, DA024044 and DE017782) for financial support. We would like to thank Theresa Nahreini for help with cell lines and flow cytometry, and John Evans for providing RAW cells.

Keywords: inhibitors · myeloid differentiation factor 2 · protein–protein interactions · structure–activity relationships · toll-like receptors

[1] P. Matzinger, *Science* **2002**, *296*, 301.
[2] L. H. Guo, H. J. Schluesener, *Cell. Mol. Life Sci.* **2007**, *64*, 1128.
[3] S. Akira, S. Uematsu, O. Takeuchi, *Cell* **2006**, *124*, 783.
[4] K. Takeda, S. Akira, *Semin. Immunol.* **2004**, *16*, 3.
[5] J. A. DeLeo, F. Y. Tanga, V. L. Tawfik, *Neuroscientist* **2004**, *10*, 40.
[6] M. R. Hutchinson, Y. Zhang, K. Brown, B. D. Coats, M. Shridhar, P. W. Sholar, S. J. Patel, N. Y. Crysdale, J. A. Harrison, S. F. Maier, K. C. Rice, L. R. Watkins, *Eur. J. Neurosci.* **2008**, *28*, 20.
[7] C. G. Leon, R. Tory, J. Jia, O. Sivak, K. M. Wasan, *Pharm. Res.* **2008**, *25*, 1751.
[8] H. Cao, Y. Q. Zhang, *Neurosci. Biobehav. Rev.* **2008**, *32*, 972.
[9] J. A. De Leo, V. L. Tawfik, M. L. LaCroix-Fralish, *Pain* **2006**, *122*, 17.
[10] S. Lehnardt, L. Massillon, P. Follett, F. E. Jensen, R. Ratan, P. A. Rosenberg, J. J. Volpe, T. Vartanian, *Proc. Natl. Acad. Sci. USA* **2003**, *100*, 8514.
[11] F. Y. Tanga, V. Raghavendra, J. A. DeLeo, *Neurochem. Int.* **2004**, *45*, 397.
[12] F. Y. Tanga, N. Nutile-McMenemy, J. A. DeLeo, *Proc. Natl. Acad. Sci. USA* **2005**, *102*, 5856.
[13] R. Shimazu, S. Akashi, H. Ogata, Y. Nagai, K. Fukudome, K. Miyake, M. Kimoto, *J. Exp. Med.* **1999**, *189*, 1777.
[14] H. Yang, D. W. Young, F. Gusovsky, J. C. Chow, *J. Biol. Chem.* **2000**, *275*, 20861.
[15] A. Visintin, E. Latz, B. G. Monks, T. Espevik, D. T. Golenbock, *J. Biol. Chem.* **2003**, *278*, 48313.
[16] B. Schnabl, K. Brandl, M. Fink, P. Gross, K. Taura, E. Gäbele, C. Hellerbrand, W. Falk, *Biochem. Biophys. Res. Commun.* **2008**, *376*, 271.
[17] C. Nishitani, H. Mitsuzawa, H. Sano, T. Shimizu, N. Matsushima, Y. Kuroki, *J. Biol. Chem.* **2006**, *281*, 38322.
[18] H. M. Kim, B. S. Park, J. I. Kim, S. E. Kim, J. Lee, S. C. Oh, P. Enkhbayar, N. Matsushima, H. Lee, O. J. Yoo, J. O. Lee, *Cell* **2007**, *130*, 906.
[19] I. Bronstein, J. Fortin, P. E. Stanley, G. S. Stewart, L. J. Kricka, *Anal. Biochem.* **1994**, *219*, 169.
[20] M. Ojaniemi, V. Glumoff, K. Harju, M. Liljeroos, K. Vuori, M. Hallman, *Eur. J. Immunol.* **2003**, *33*, 597.
[21] J. H. Evans, J. J. Falke, *Proc. Natl. Acad. Sci. USA* **2007**, *104*, 16176.
[22] B. Bacsa, C. O. Kappe, *Nat. Protoc.* **2007**, *2*, 2222.
[23] C. A. Rohl, C. E. Strauss, K. M. Misura, D. Baker, *Methods Enzymol.* **2004**, *383*, 66.
[24] B. Kuhlman, D. Baker, *Proc. Natl. Acad. Sci. USA* **2000**, *97*, 10383.
[25] G. Dantas, C. Corrent, S. L. Reichow, J. J. Havranek, Z. M. Eletr, N. G. Isern, B. Kuhlman, G. Varani, E. A. Merritt, D. Baker, *J. Mol. Biol.* **2007**, *366*, 1209.
[26] R. L. Dunbrack, Jr., F. E. Cohen, *Protein Sci.* **1997**, *6*, 1661.

Received: November 22, 2008
Published online on January 30, 2009

